An assessment of the effect of horizontal soil moisture heterogeneity on the area-average measurement of cosmic-ray neutrons

Trenton E. Franz,[1,2] M. Zreda,[1] T. P. A. Ferre,[1] and R. Rosolem[1,3]

Received 5 March 2013; revised 10 September 2013; accepted 12 September 2013.

[1] The cosmic-ray neutron probe measures soil moisture over tens of hectares, thus averaging spatially variable soil moisture fields. A previous paper described how variable soil moisture profiles affect the integrated cosmic-ray neutron signal from which depth-average soil moisture is computed. Here, we investigate the effect of horizontal heterogeneity on the relationship between neutron counts and average soil moisture. Observations from a distributed sensor network at a site in southern Arizona indicate that the horizontal component of the total variance of the soil moisture field is less variably in time than the vertical component. Using results from neutron particle transport simulations we show that 1-D binary distributions of soil moisture may affect both the mean and variance of neutron counts of a cosmic-ray neutron detector placed arbitrarily in a soil moisture field, potentially giving rise to an underestimate of the footprint average soil moisture. Similar simulations that used 1-D and 2-D Gaussian soil moisture fields indicate consistent mean and variances of a randomly placed detector if the correlation length scales are short (less than ~30 m) and/or the soil moisture field variance is small (<0.032 m^6 m^{-6}). Taken together, these soil moisture observations and neutron transport simulations show that horizontal heterogeneity likely has a small effect on the relationship between mean neutron counts and average soil moisture for soils under natural conditions.

Citation: Franz, T. E., M. Zreda, T. P. A. Ferre, and R. Rosolem (2013), An assessment of the effect of horizontal soil moisture heterogeneity on the area-average measurement of cosmic-ray neutrons, *Water Resour. Res.*, *49*, doi:10.1002/wrcr.20530.

1. Introduction

[2] With the continued development of high-resolution land surface models [*Wood et al*., 2011], there is a great need for standardized, high-quality, and high-resolution soil moisture data sets. Given the large horizontal footprint of the cosmic-ray neutron probe at tens of hectares [*Desilets and Zreda*, 2013] and its effective measurement depth of tens of centimeters [*Zreda et al*., 2008], the probe is an ideal candidate for model calibration and validation. With the long-term deployment of 50 probes around the continental USA—and eventual expansion to 500—the COsmic-ray Soil Moisture Observing System (COSMOS, data available at http://cosmos.hwr.arizona.edu/) [*Zreda et al*. 2012] has the potential to provide some of these required high-resolution soil moisture data sets.

[3] The cosmic-ray neutron probe is sensitive to all hydrogen atoms in the measurement volume [*Desilets et al*., 2010]. Previous publications have evaluated the effects of water vapor [*Rosolem et al*., 2013], growing vegetation [*Hornbuckle et al*., 2012], and 1-D wetting and drying cycles in porous media [*Franz et al*., 2012a] on measured neutron counts. In this paper, we explore the potential effects due to horizontal soil moisture heterogeneity inside the ~28 ha measurement area. At this spatial scale, soil texture, soil structure, and topography may all play critical roles on the organization of soil moisture [*Crow et al*., 2012, Figure 1], whereas hydroclimatic factors are likely less important. Observations [*Crow et al*., 2012; *Famiglietti et al*., 2008] and modeling of porous media [*Vereecken et al*., 2007] suggest an inverted parabolic relationship between the mean and standard deviation of soil moisture. This spatial heterogeneity has been used to estimate soil hydraulic properties through inverse stochastic modeling [*Vereecken et al*., 2007]. However, this inherent spatial heterogeneity makes comparison of footprint-scale soil moisture and sparse ground-based observations difficult [*Crow et al*., 2012].

[4] The objective of this work is to investigate how the spatial organization of soil moisture may affect cosmic-ray neutron probe measurements and subsequent estimation of area-average soil moisture. The key assumption of the cosmic-ray neutron method is that low-energy neutrons (defined here as neutrons between 1 and 1000 eV, see section 2.2) above the soil-atmospheric interface form a well-mixed reservoir because (1) the velocity of low-energy neutrons have velocities of tens to thousands of kilometers per second [*Zreda et al*., 2012], (2) the collision mean free path

[1]Department of Hydrology and Water Resources, University of Arizona, Tucson, Arizona, USA.
[2]Now at School of Natural Resources, University of Nebraska-Lincoln, Lincoln, Nebraska, USA.
[3]Now at Department of Civil Engineering, University of Bristol, Bristol, UK.

Corresponding author: T. E. Franz, School of Natural Resources, University of Nebraska-Lincoln, 607 Hardin Hall, Lincoln, NE 68583, USA. (tfranz2@unl.edu)

0043-1397/13/10.1002/wrcr.20530

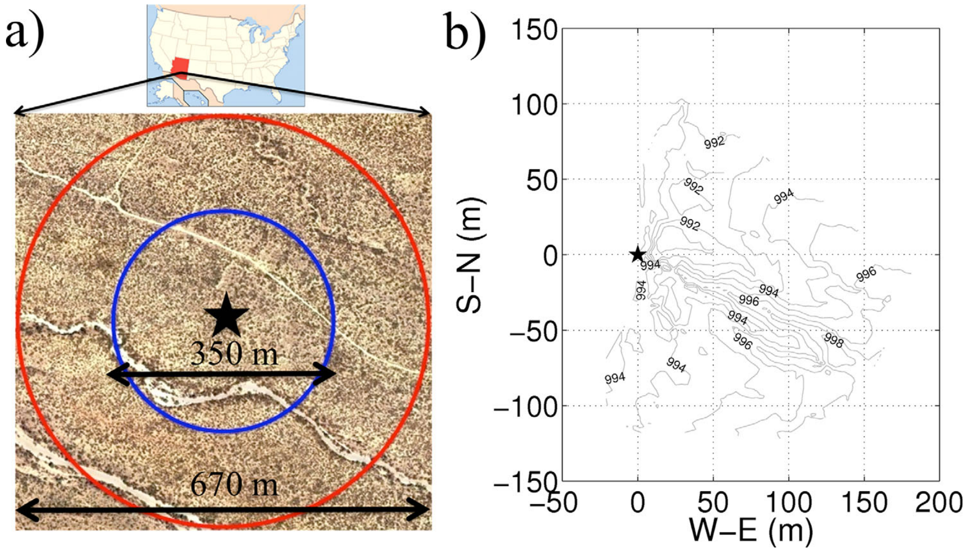

Figure 1. (a) Location of the cosmic-ray neutron probe (black star, 31.9085°N 110.8394°W) and horizontal footprint (blue and red ellipses are 63% and 86% cumulative sensitivity contours) in southern Arizona at SRER and (b) elevation contours (m) inside part of the study area. Modified from *Franz et al.*, [2012b, Figure 1].

of low-energy neutrons in air is ∼30 m [*Desilets*, 2011], and (3) during the scattering process the low-energy neutrons on average go through 20 to 60 collisions [*Desilets*, 2011]. Here we describe various degrees of heterogeneous soil moisture fields where the mean neutron count rate is either representative or not of the area-average soil moisture.

[5] In this work, we present a suite of near surface soil moisture observations derived from geophysical instruments in a semiarid shrubland in southern Arizona to characterize the spatiotemporal soil moisture patterns. Using a distributed sensor network, we present a time series of area-average soil moisture inside the cosmic-ray neutron probe footprint. In addition, we present neutron particle transport modeling results that show neutron intensities under prescribed, hypothetical soil moisture heterogeneities in 1-D and 2-D.

2. Methodology

[6] The methods section starts with a description of the study site in southern Arizona, section 2.1, where two different geophysical methods were used to estimate near surface soil moisture. Section 2.2 describes the cosmic-ray neutron method for estimating continuous area-average soil moisture and section 2.3 describes continuous point measurements using time-domain-transmission probes in a distributed sensor network. The last section, 2.4, describes the neutron particle transport code used to simulate the response of the cosmic-ray neutron probe to different site conditions.

2.1. Study Site

[7] Soil moisture was measured with two different geophysical techniques at the Santa Rita Experimental Range (SRER) in southern Arizona (31.9085°N 110.8394°W, Figure 1a) [*Franz et al.*, 2012b]. The mean annual rainfall at SRER is ∼400 mm, with 50% occurring between July and September [*Scott et al.*, 2008]. Actual evapotranspiration ranges from 3 mm day^{-1} to 4 mm day^{-1} in summer months (June–September) and from ∼0 mm day^{-1} to 2 mm day^{-1} during winter months (December–February) [*Cavanaugh et al.*, 2011; *Scott et al.*, 2008]. The vegetation at SRER is composed primarily of creosotebush (∼14% by area), with some grasses, forbes, catci, and mesquite (∼10% by area) [*Cavanaugh et al.*, 2011]. *Cavanaugh et al.* [2011] characterized the soils as Agustin sandy loam with 5% to 15% gravel in the top meter, and having a relatively deep caliche layer (>1 m). The landscape consists of long narrow subcatchments and has an average slope of 2° (Figure 1b).

2.2. Area-Average Soil Moisture Measurements Using a Cosmic-Ray Neutron Probe

[8] A cosmic-ray neutron probe (Model CRS-1000 from Hydroinnova LLC, Albuquerque, NM) was installed at the study site on 2 June 2010 as part of the COSMOS network [*Zreda et al.*, 2012]. *Zreda et al.* [2012] provides a comprehensive summary of cosmic-ray physics, the cosmic-ray neutron probe, and the method used to quantify soil moisture using low-energy neutron counts. Here we use the moderated or fast neutron detector at SRER to quantify soil moisture. The moderated neutron detector is shielded by 2.5 cm of plastic making it most sensitive to neutrons between 1 eV and 1000 eV with a median energy of 10 eV [*Desilets*, 2011; *Knoll*, 2000]. We note from neutron transport modeling that the relationship between average hydrogen content and neutron flux is nearly identical over these energy ranges.

[9] *Desilets et al.* [2010] developed a nonlinear calibration function that relates average volumetric water content to moderated neutron counts

$$\theta(N) = \frac{0.0808}{\left(\frac{N}{N_0}\right) - 0.372} - 0.115 \tag{1}$$

where θ (m^3 m^{-3}) is the average volumetric water content, N is the moderated neutron counting rate (count h^{-1}, cph) normalized to a reference atmospheric pressure and solar activity level [*Zreda et al*., 2012], and N_0 (cph) is the moderated counting rate over dry soil under the same reference conditions and needs to be estimated with at least one independent soil moisture calibration. *Franz et al*. [2012b] performed a detailed analysis of N_0 at SRER and found it varied between a minimum value of 3100 and maximum value of 3300 cph for five different calibration datasets, resulting in an RMSE = 0.0165 $m^3\ m^{-3}$ when comparing it to independent soil moisture estimates from a distributed sensor network.

[10] Using neutron particle transport modeling *Zreda et al*. [2008] found that the probe has a horizontal support of ~28 ha (a circle with radius 300 m at sea level in a dry atmosphere). More recently *Desilets and Zreda* [2013] found the support radius is reduced by 20 m per additional 10 g of water per kg of air but does increase with elevation above sea level. *Zreda et al*. [2008] also indicates the vertical support ranges from 12 cm in saturated soils to 70 cm in hydrogen free soils. However, *Zreda et al*. [2012] found that background soil water in the continental USA (sum of lattice water and soil organic carbon water equivalent) varies between 0.01 gg^{-1} and 0.10 gg^{-1} thus reducing the effective vertical depth to ~30–40 cm in dry soils (no pore water). Building on this work, *Franz et al*. [2012a] coupled a solution to the 1-D Richards equation with the neutron particle transport model and derived an expression for the vertical support of the probe given uniform and vertically variable soil moisture profiles. Due to the different vertical distribution of soil moisture between wetting and drying cycles, *Franz et al*. [2012a] found that the relationship between neutron counts and average soil moisture was nonunique, and that the size of the resulting hysteretic loop was largest for coarse textured soils in which sharp wetting fronts may exist following precipitation. For finer textured soils *Franz et al*. [2012a] found the nonuniqueness to be minimal.

2.3. Continuous Soil Moisture Measurements Using a Distributed Sensor Network

[11] Depth profiles of time-domain transmission probes (TDT: Model ACC-SEN-TDT from Acclima Inc., Meridian, ID) were installed at 18 different points around the COSMOS probe: six transects in the horizontal directions from 0° to 300° every 60°, each with three radii of 25 m, 75 m, and 200 m (see *Franz et al*. [2012b] for exact locations and full experiment details). Given the horizontal sensitivity of the cosmic-ray neutron probe [*Zreda et al*., 2008], each location was selected such that each subarea would have equal weight when averaging soil moisture over the horizontal. Between 15 and 26 June 2011, TDT probes were inserted horizontally at 10, 20, 30, 50, and 70 cm depths in open areas and beneath a creosotebush within 3 m of each other at each of the 18 locations. One additional probe at 5 cm was added to each profile on 5 January 2012 to capture soil moisture behavior near the surface. The probes were inserted horizontally following excavation of a 1 m^3 soil pit. A chisel of the same dimensions as the TDT probe was used to excavate a cavity in the upslope soil face. The TDT probe was then placed in the cavity using the excavated soil to backfill the remaining void space. After all TDT probes were in place we repacked the excavated soil pit using the soil from the same depth and location in order to recreate the observed soil bulk density as best as possible.

[12] Acclima TDT probes have been shown to have performance equivalent to conventional time-domain reflectometry [*Blonquist et al*., 2005]. *Franz et al*. [2012b] found from laboratory and field calibration with volumetric samples that the TDT probes had on average a measurement uncertainty of less than 0.02 $m^3\ m^{-3}$. When comparing the weighted average from the TDT data with the cosmic-ray neutron probe *Franz et al*. [2012b] found an RMSE = 0.0165 $m^3\ m^{-3}$, with maximum absolute deviations around 0.03 $m^3\ m^{-3}$ at peak soil moisture values following rain events.

2.4. Neutron Particle Transport Modeling

[13] We used the Monte Carlo N-Particle eXtended model (MCNPx) [*Pelowitz*, 2005] to simulate transport of neutrons throughout the atmosphere and near the land surface. MCNPx is a general purpose Monte Carlo model that simulates the life history of an individual particle and its consequent particles as it interacts with different elements. Starting at 8 km above the surface, we simulated a source of neutrons oriented downward with a randomly selected starting energy and location over a 1.2 km × 1.2 km domain with periodic boundary conditions (a neutron leaving the domain is reinserted on the opposite side with the same energy level in order to complete its life history), as consistent with previous work [*Franz et al*., 2012a; *Zreda et al*., 2008]. We assumed the atmosphere was composed of dry air and followed standard lapse rates starting at sea level. We assumed the subsurface was composed of 4 m deep silica sand (SiO_2) with a dry bulk density of 1.4 g cm^{-3}. The small numbers of particles making it below 4 m in the subsurface were removed from the simulations, as they do not affect the simulation results of low-energy neutron counts above the surface.

[14] In contrast to previous work that considered only 1-D vertical heterogeneity [*Franz et al*., 2012a; *Zreda et al*., 2008], here we investigate the response of low-energy neutrons to 1-D and 2-D horizontal heterogeneity. We placed 10 m × 10 m × 1200 m box detectors, starting at 0.5 m above the surface, every 50 m between 300 and 900 m in the domain. Each detector records the approximate moderated neutron flux. Here we tally neutrons with energy levels between 10 eV and 100 eV, which corresponds to the energy level of the moderated channel (see section 2.2). In order to achieve a standard error of the mean less than 2% for each detector (same error level as previous modeling work and equal to an observed error at the counting level of ~2500 cph), we simulated 30 million particle life histories for each model run. For each set of simulations we normalize the moderated neutron flux, N, to the moderated neutron flux over liquid water, N_S, where the soil in the subsurface is replaced with liquid water. Therefore, for a given instrument and site-specific N_S value, the actual neutron count rate can be computed. For this work, we assume $N_S \sim 1000$ cph, which was estimated from previous site-specific instrument calibrations [*Franz et al*., 2013]. We note that equation (1) and the derived more general relationships in *Franz et al*. [2013] will be nearly identical for a specific site where all hydrogen pools are specified.

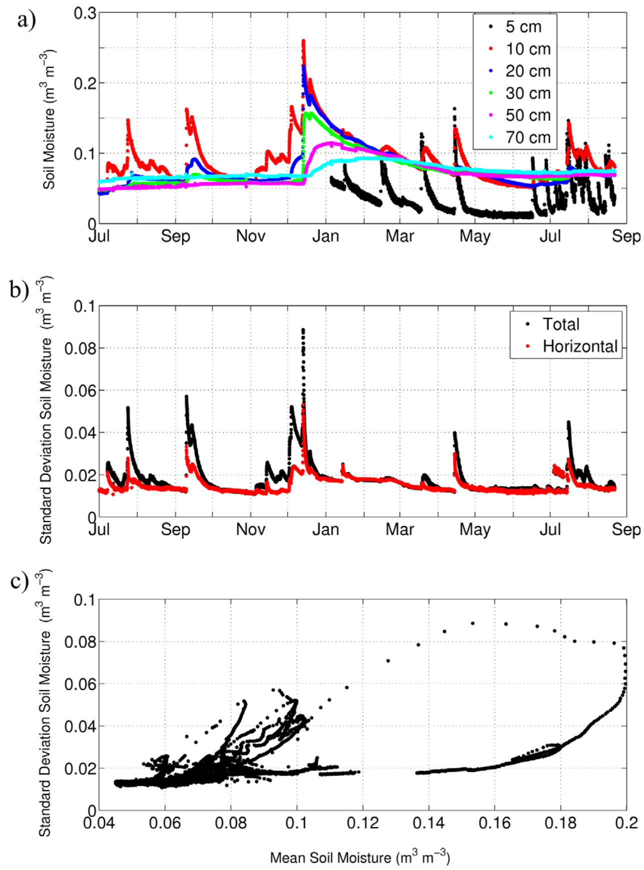

Figure 2. (a) Hourly horizontally averaged TDT data by depth at SRER between July 2011 and September 2012. (b) Total (black), and horizontal (red) components of the standard deviation of the soil moisture field between 0 and 30 cm. (c) Relationship between the mean and standard deviation of soil moisture between 0 and 30 cm. Note only the 10, 20, and 30 cm probe were used to compute the mean and standard deviation for the entire time series.

3. Results

3.1. Observed Continuous Soil Moisture Patterns

[15] The time series of soil moisture profiles (Figure 2a) from the TDT sensors show two contrasting behaviors. First, during summer months (June–September) the soil moisture dynamics are confined to the top 20 cm of the soil and deep infiltration is absent. As expected, the probe at 5 cm is consistently lower than the other probes, indicating strong evaporation at the soil surface. Second, during winter months (December–February) soil moisture variations in time extend to the depth of 70 cm. This is due to low evapotranspiration that permits deep infiltration.

[16] During infiltration events, we find the total standard deviation (computed as the standard deviation of all probes at depths of 10, 20, and 30 cm, shown by upper limb of black dots in Figure 2c) of the soil moisture field increases with mean soil moisture. We also find the upper limb approximately follows the inverted parabolic shape reported elsewhere between the mean and standard deviation of soil moisture [*Famiglietti et al.*, 2008; *Vereecken et al.*, 2007] (Note that the maximum mean soil moisture at SRER is only 0.20 $m^3 m^{-3}$ so only the increasing part of the inverted parabola is shown). However, we do find that after peak soil moisture for a given rain event, the total standard deviation decays faster and hysteretically during drainage as compared to infiltration (Figure 2c) as suggested by homogenization affects due to vegetation [*Ivanov et al.*, 2010]. By computing the vertical component of the total standard deviation (computed as the standard deviation of the 10, 20, and 30 cm layer averages), the remaining horizontal component can be isolated (red dots in Figure 2b). The nonzero baseline of the horizontal standard deviation likely is influenced by the level of soil texture variability present at the 18 different profile locations around the footprint. During extended dry periods, the total standard deviation approaches the horizontal value indicating the lack of vertical heterogeneity due to soil drying to uniform low moisture content in the top 30 cm. We note that we slightly underestimate the total and vertical standard deviation of the top 30 cm as some of the surface soil moisture will be missed by the 10 cm probes.

3.2. Modeled Neutron Response to 1-D Horizontal Heterogeneity

[17] Using MCNPx, we investigated how 1-D horizontal heterogeneity of soil moisture affects the neutron counts. The heterogeneous soil moisture fields were created using different methods. First, stripes of soils with different sizes and alternating moisture values were created. This was the simplest heterogeneity investigated in this work. More complex heterogeneities were created using stochastic methods based on Gaussian random fields and produced the most realistic distribution of soil moisture.

[18] One-dimensional heterogeneity was made of alternating dry (soil moisture of 0.05 $m^3\ m^{-3}$) and wet (0.35 $m^3\ m^{-3}$) stripes that extend across the modeling domain in one direction, and that have variable second dimension—from 2 m to 600 m. Neutron intensity for simulated detectors placed every 50 m between 300 and 900 m was calculated for each geometry along a center line going across the domain in the direction perpendicular to the stripes. These neutron intensities were then converted to equivalent uniform soil moisture values using equation (1). The input soil moisture fields (left column), modeled neutron intensities (center column), and modeled soil moistures (right column) are shown in Figure 3. The top row in Figure 3 shows the configuration with the narrow stripes 50 m wide, the middle row is for 150 m wide stripes, and the bottom for 600 m wide stripes. With increasing stripe size, the deviations of the modeled neutron counts at each detector vary systematically until we reach the step-like function for a probe footprint radius of ~300 m. Given the nonlinear relationship between neutron counts and soil moisture (equation (1)), the sharp decrease in modeled neutron counts is evident as the detectors approach the step function in the soil moisture field (Figure 3, bottom row). Whereas the local detectors are consistent with the average neutron conditions over the footprint radius, the nonlinearity in equation (1) may lead to average soil moisture values that are too low compared to the actual soil moisture field. We note that while this exercise was useful in establishing the importance of horizontal heterogeneity, this geometry is unrealistic and results in an overestimate of the influence of the

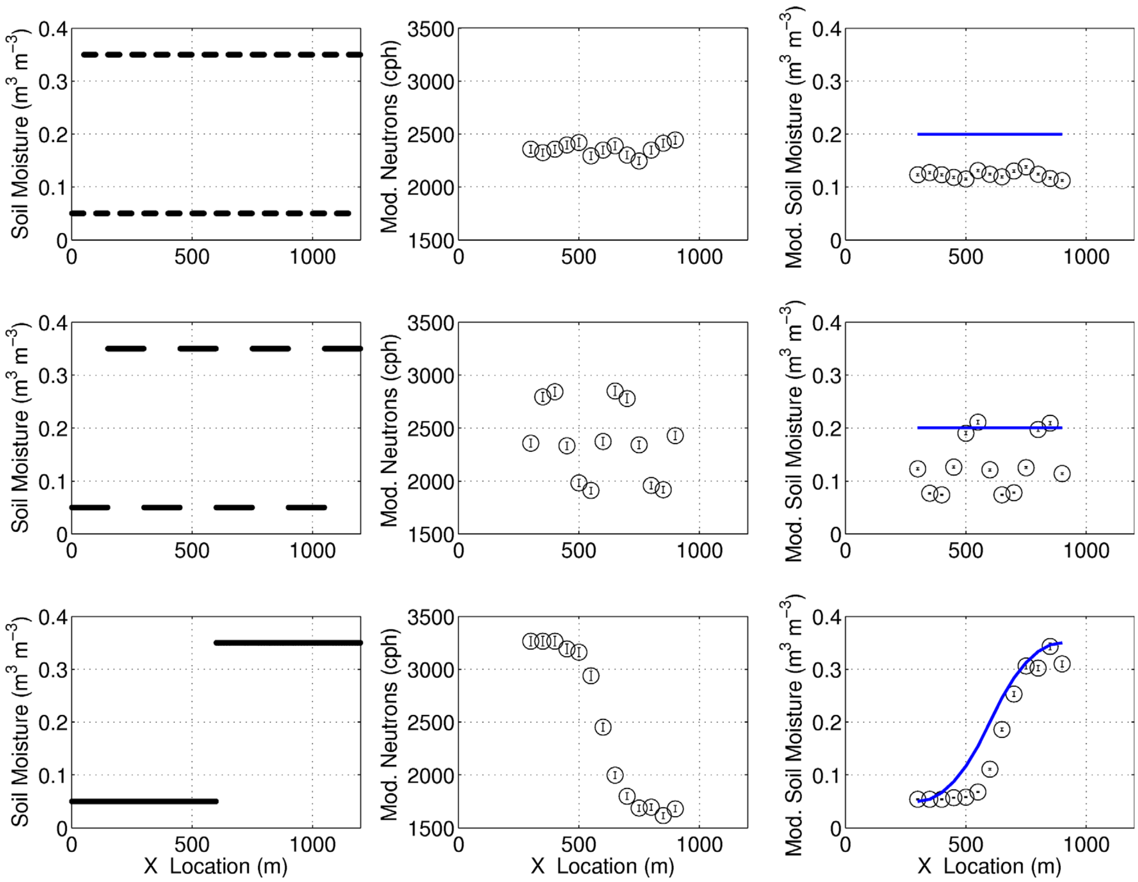

Figure 3. Hypothetical cases of binary wet and dry stripes of varying length (left column), modeled neutron counts (middle column), and estimated soil moisture along domain (right column). Error bars are 1 standard error of the mean flux value from the MCNPx modeling and the blue lines are 600 m window averages of the soil moisture field.

distribution of neutron intensity and therefore it is useful to look at more realistic soil moisture distribution scenarios.

[19] In addition to using uniform soil moisture stripes, we investigated more realistic 1-D soil moisture fields by creating stripe widths and soil moisture values using random Gaussian fields with known mean, variance, and correlation length. Figure 4 shows the results from two dry (mean 0.05 m^3 m^{-3}, variance 0.022 m^6 m^{-6}, rows 1 and 2) and wet cases (0.30 m^3 m^{-3}, 0.055 m^6 m^{-6}, rows 3 and 4) for two different correlation lengths (2 m and 100 m). As with the uniform stripes, also here the modeled neutron counts are affected by the location of the detector and the surrounding soil moisture field; with longer correlation lengths (Figure 4, rows 2 and 4) resulting in larger neutron count variations. But there is a difference between the two geometries. In the case of uniform stripe widths, neutron-derived soil moisture showed a consistent negative bias everywhere in the domain (right column in Figure 3). In contrast, here neutron-derived soil moisture had no such bias (right column in Figure 4). The modeled oscillations at a detector reflect the local soil moisture field when averaging over a 600 m window around the detector location as shown by the blue line in Figure 4.

[20] Generalizing the various 1-D cases, we plot the modeled response of the probe to various uniform binary and Gaussian soil moisture fields (Figure 5). Here the x axis is the characteristic length of the soil moisture field (either stripe width for uniform binary cases or correlation length for Gaussian fields) divided by the footprint radius. The y axis is the neutron deviation, maximum neutron count minus minimum neutron count divided by expected neutron count for a given soil moisture, for a randomly placed box detector in the field (along axis in 1-D). The neutron deviation grows with increasing normalized characteristic length approaching its maximum value near 1. As expected, the largest neutron count deviation is for the uniform binary case with the largest soil moisture spread, the binary distribution B[0.05, 0.35 m^3 m^{-3}] that assumes values of 0.05 m^3 m^{-3} and 0.35 m^3 m^{-3} only. For the B[0.15, 0.25 m^3 m^{-3}] case, the magnitude of the neutron deviation is greatly reduced. The Gaussian soil moisture cases have smaller neutron deviations comparatively to uniform binary cases, where B[0.05, 0.35 m^3 m^{-3}] and N(0.20 m^3 m^{-3}, 0.045 m^6 m^{-6}) have a similar spread of soil moisture values. For the Gaussian fields with variances of 0.022 and 0.032 m^6 m^{-6} and normalized characteristic lengths less than ~0.10 (equal to a correlation length of 30 m), the neutron deviations are not statistically different from the numerical uncertainty in the MCNPx modeling.

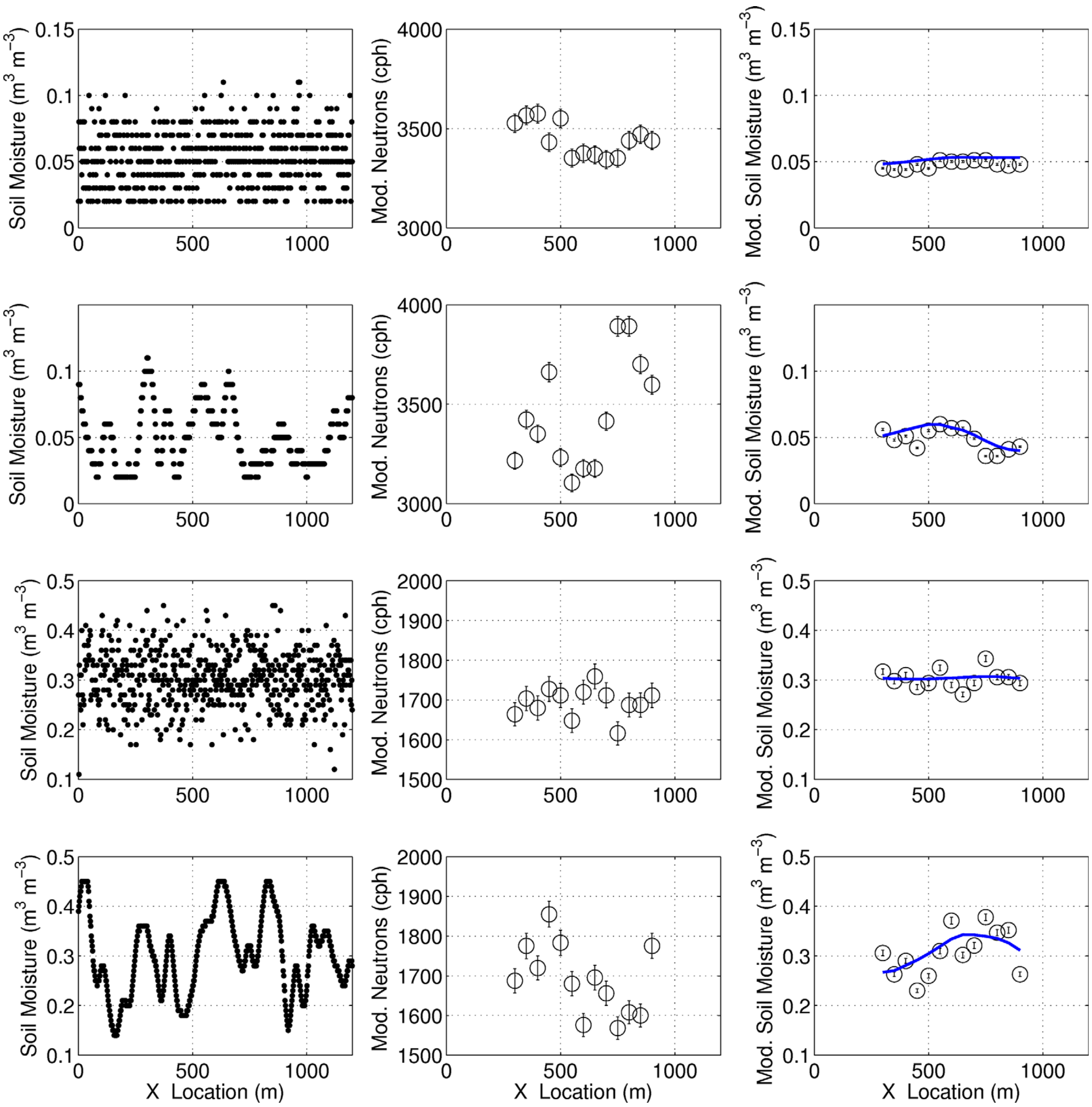

Figure 4. Hypothetical cases of dry (mean 0.05 m^3 m^{-3}, variance 0.022 m^6 m^{-6}, rows 1 and 2) and wet (mean 0.30 m^3 m^{-3}, variance 0.055 m^6 m^{-6}, rows 3 and 4) stripes with varying correlation lengths (2 and 100 m) (left column), modeled neutron counts (middle column), and estimated soil moisture along domain (right column). Error bars are 1 standard error of the mean flux value from the MCNPx modeling and the blue lines are 600 m window averages of the soil moisture field.

3.3. Modeled Neutron Response to 2-D Horizontal Heterogeneity

[21] We investigated two hypothetical 2-D cases using checkerboards with varying grid sizes. The first case was for binary soil moisture values and the second for soil moisture values drawn from a Gaussian distribution specified by a mean and variance. Figure 6 compares the 1-D and 2-D modeling results in terms of the mean modeled neutron counts and standard deviation of modeled neutron counts for a randomly placed box detector along an axis. For the 1-D binary stripe cases, (stripe sizes 2, 4, 10, 20, 30, 40, 50, 60, 100, 150, 200, 300, and 600 m) both the mean and standard deviation of modeled neutron counts are functions of the stripe width. In addition, the mean modeled neutron counts are larger for the binary case B[0.05, 0.35 m^3 m^{-3}] as compared to B[0.15, 0.25 m^3 m^{-3}], despite having the same mean field soil moisture value. This difference in mean modeled counts is due to averaging the nonlinear function of soil moisture versus neutron counts (equation (1)) for heterogeneous fields: dry soils correspond to very high neutron counts and have a disproportionately large effect on the neutron count leading to underestimates of average soil moisture for the footprint.

[22] In the 2-D binary checkerboard cases (checkerboard side sizes 50, 100, 200, 300, and 600 m), the absolute difference in the mean modeled counts between the B[0.05, 0.35 m^3 m^{-3}] and B[0.15, 0.25 m^3 m^{-3}] cases is clearly discernible. However, the standard deviations are similar

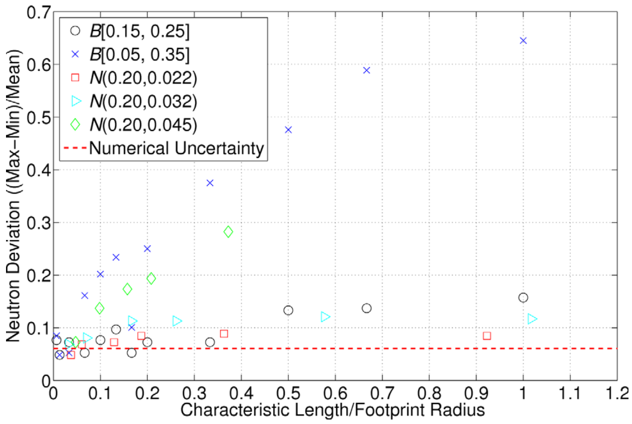

Figure 5. Modeled probe response for a randomly placed box detector in 1-D binary and Gaussian soil moisture fields with the same mean field soil moisture value. The magnitude of the neutron deviation grows as the characteristic length (either stripe size or correlation length) of the soil moisture field approaches the footprint radius of ~300 m. For short characteristic lengths, the neutron deviation is small and not statistically different from the numerical model uncertainty. Note the mean value in the y axis neutron deviation is the expected count rate of 1974 cph for a homogeneous soil moisture field at 0.20 m^3 m^{-3}.

and are not a function of the checkerboard side distance, which is in stark contrast to the geometries involving stripes. Finally, for the checkerboard with soil moisture values drawn from a Gaussian distribution, N(0.20 m^3 m^{-3}, 0.022 m^6 m^{-6}) and N(0.20 m^3 m^{-3}, 0.045 m^6 m^{-6}), the mean modeled neutron values and their standard deviations are similar and do not depend on checkerboard side distance.

4. Discussion

4.1. A General Relationship Between Neutrons and Horizontal Soil Moisture Fields

[23] Because the relationship between neutron counts and soil moisture is nonlinear (equation (1)), heterogeneous soil moisture conditions may lead to different neutron count rates for the same field average soil moisture (Figure 6). By extension, it can be conjectured that the same neutron count rate can be measured for different average soil moisture fields. Here we have identified soil moisture patterns where both the mean and standard deviation of modeled neutron counts depend on the spatial structure of the soil moisture field. These obfuscating cases were simulated for uniform binary soil moisture fields in 1-D and 2-D, which are not realistic representations of field conditions. In contrast, Gaussian soil moisture fields did not exhibit this behavior (Figures 5 and 6). Simulations of 1-D Gaussian fields showed consistent behavior of locally measured neutrons and conversation to average soil moisture with that of a 600 m window average of the true soil moisture field (Figure 4).

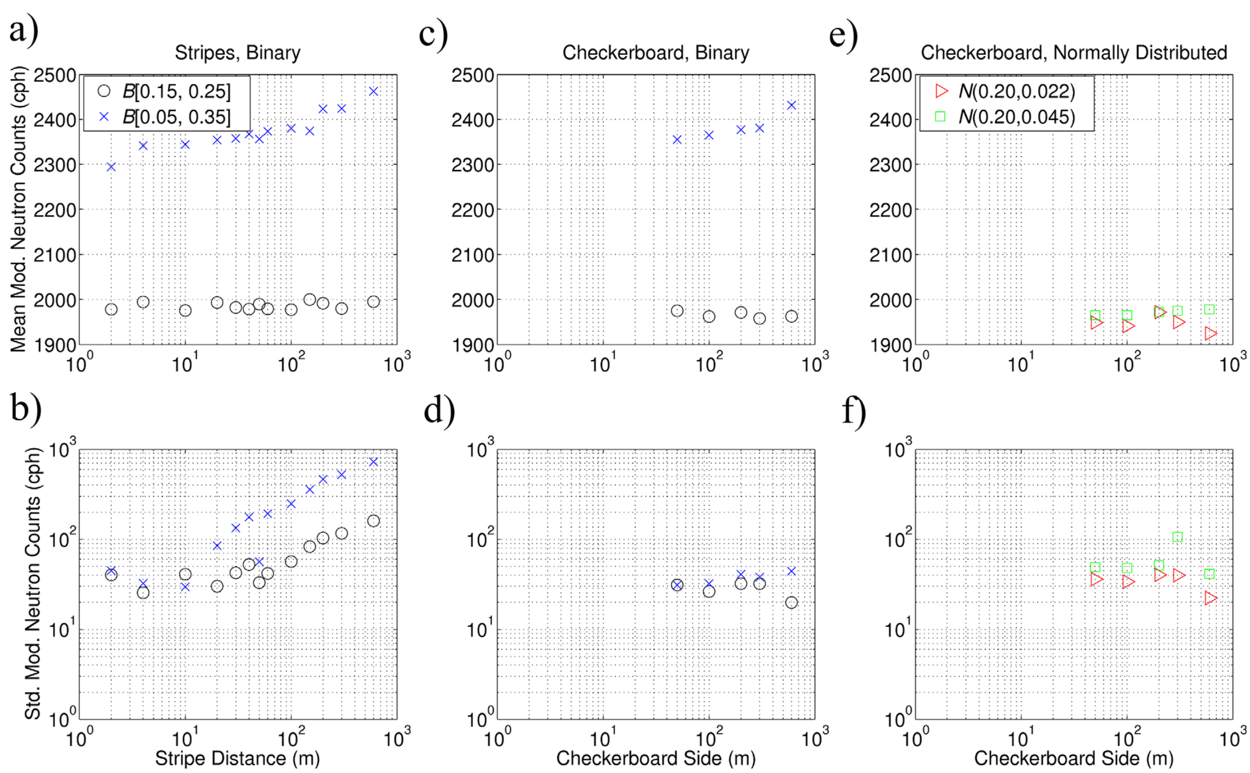

Figure 6. Mean and standard deviation of modeled neutron counts for a randomly placed box detector with varying spatial correlation lengths for (a and b) striped binary, (c and d) checkerboard binary, and (e and f) checkerboard Gaussian distributed soil moisture field. Note the expected neutron count for a homogenous soil moisture field at 0.20 m^3 m^{-3} is 1974 cph.

4.2. General Soil Moisture Patterns Observations From SRER

[24] We have characterized the soil moisture field at SRER using two geophysical methods, TDT probes and a cosmic-ray neutron probe, and combined the field data with neutron particle transport modeling to investigate the impact of horizontal heterogeneity of soil moisture on neutron counts. The TDT data show that the total standard deviation of the soil moisture field increases with the mean soil moisture (Figure 2b). By decomposing the standard deviation into the vertical and horizontal component, we are able to investigate the temporal stability of the calibration parameter N_0. Because the N_0 value in equation (1) is typically calibrated with local samples, the horizontal component of the standard deviation will be implicitly accounted for in the calibration function. That means that if the horizontal component of variation is not changing significantly in time, N_0 will not be a function of the mean of the soil moisture field. TDT data from SRER indicate that the horizontal component of the standard deviation varies between 0.01 and 0.05 m^3m^{-3}, which is likely to cause only minor deviations in the N_0 value and mean soil moisture estimates as computed with MCNPx from hypothetical soil moisture fields (data not shown here). We also note for the short periods following rain events, the total standard deviation may be large due to soil moisture differences with depth (infiltration fronts). For these periods, we also recommend vertical averaging of the profile (instead of simple arithmetic averages) following equations in *Franz et al*. [2012a] in order to account for the potential hysteresis.

4.3. Placement of Neutron Detectors in Heterogeneous Fields

[25] Placement of cosmic-ray neutron probes in heterogeneous fields should prescribe to the following suggestions based on MCNPx modeling and observed heterogeneity at SRER. For cases of 1-D heterogeneity, locally dry stripes may result in average neutron counts that are too high, resulting in too low average soil moisture. In addition, as the individual stripe lengths exceed 10 m (Figure 6), the standard deviation of neutron counts increases with stripe size making placement of the detector in this random field sensitive to small-scale conditions.

[26] While these types of conditions are unlikely in nature, irrigated fields and urban environments (for example those with wide roads) may contain soil moisture fields approaching this structure of heterogeneity. For such conditions, the calibration function will be different than that in equation (1). To accommodate this change, we recommend defining a local calibration function using multiple calibration data sets at different soil moisture values or using MCNPx and local site conditions to define a unique, local calibration function.

[27] For natural ecosystems, local wet and dry patches may exist given the spatial distribution of soil texture and site topography, as observed at SRER and described elsewhere [*Crow et al*., 2012]. Simulations of 1-D Gaussian fields suggest that observed neutron counts will be largely insensitive to soil moisture fields with short correlation length scales, less than ~30m (Figures 4 and 5). Placement or movement of the probe in locally wet or dry areas may result in small neutron count differences, but the differences would be reflected in the local averaging of the soil moisture field (a window average of ~600 m).

[28] Two-dimensional binary soil moisture fields may affect average neutron counts. However, this is not true for the more realistic soil moisture fields with Gaussian distributed values. Time-lapse electromagnetic induction surveys at SRER suggest the soil moisture field has a near Gaussian distribution following rain events. Repeated calibration data sets of N_0 in equation (1) [*Franz et al*., 2012b] and the small value of the horizontal component of the standard deviation of the soil moisture field (Figure 2b) suggest the soil moisture patterns at SRER do not cause large deviations in the local calibration function. Future work should focus on the temporal stability of the calibration parameter N_0 at other cosmic-ray probe sites, the quantification of the horizontal component of the standard deviation of the soil moisture field, and the potential effects of the horizontal component of the standard deviation on the local calibration function.

5. Conclusions

[29] The work described herein has led to four conclusions:

[30] 1. Modeling simulations indicate that soil moisture fields with short correlation lengths (less than ~30 m) and/or small variances (<0.032 m^6 m^{-6}) have no significant impact on average neutron counts for a randomly placed detector in a Gaussian field.

[31] 2. Modeling simulations indicate that binary or near-binary soil moisture distributions would result in underestimates of soil moisture because the dry areas are disproportionately represented in the observed neutron counts.

[32] 3. The impact of horizontal soil moisture heterogeneity on average neutron counts and area-average soil moisture is minimal where (1) soil moisture fields are near Gaussian and (2) the variance of the soil moisture field is implicitly included in the estimate of N_0 in equation (1) and remains constant in time.

[33] 4. For special site conditions where horizontal heterogeneity has been identified as important (i.e., 1-D stripes), it is critical to establish local calibration functions with onsite sampling or numerical modeling instead of utilizing equation (1).

[34] **Acknowledgments.** This research and the COSMOS project were supported by the US National Science Foundation under grant AGS-0838491. We would like to thank Santa Rita Experimental Range for allowing us to work on site. We would also like to thank Adam Karczynski and Bobby Chrisman for helping setup and maintaining the TDT network.

References

Blonquist, J. M., S. B. Jones, and D. A. Robinson (2005), A time domain transmission sensor with TDR performance characteristics, *J. Hydrol.*, *314*(1-4), 235–245. doi:10.1016/j.jhydrol.2005.04.005.

Cavanaugh, M. L., S. A. Kurc, and R. L. Scott (2011), Evapotranspiration partitioning in semiarid shrubland ecosystems: A two-site evaluation of soil moisture control on transpiration, *Ecohydrology*, *4*(5), 671–681. doi:10.1002/eco.157.

Crow, W. T., A. A. Berg, M. H. Cosh, A. Loew, B. P. Mohanty, R. Panciera, P. de Rosnay, D. Ryu, and J. P. Walker (2012), Upscaling sparse ground-based soil moisture observations for the validation of coarse-resolution satellite soil moisture products, *Rev. Geophys.*, *50*, RG2002, doi:10.1029/2011RG000372.

Desilets, D. (2011), Radius of influence for a cosmic-ray soil moisture probe: Theory and Monte Carlo simulations, *Sandia Rep. SAND2011-1101*, Sandia Natl. Lab., Albuquerque, N. M. and Livermore, Calif.

Desilets, D., and M. Zreda (2013), Footprint diameter for a cosmic-ray soil moisture probe: Theory and Monte Carlo simulations, *Water Resour. Res.*, *49*, 3566–3575, doi:10.1002/wrcr.20187.

Desilets, D., M. Zreda, and T. P. A. Ferre (2010), Nature's neutron probe: Land surface hydrology at an elusive scale with cosmic rays, *Water Resour. Res.*, *46*, W11505, doi:10.1029/2009WR008726.

Famiglietti, J. S., D. R. Ryu, A. A. Berg, M. Rodell, and T. J. Jackson (2008), Field observations of soil moisture variability across scales, *Water Resour. Res.*, *44*, W01423, doi:10.1029/2006WR005804.

Franz, T. E., M. Zreda, P. A. Ferre, R. Rosolem, C. Zweck, S. Stillman, X. Zeng, and W. J. Shuttleworth (2012a), Measurement depth of the cosmic-ray soil moisture probe affected by hydrogen from various sources, *Water Resour. Res.*, *48*, W08515, doi:10.1029/2012WR011871.

Franz, T. E., M. Zreda, R. Rosolem, and P. A. Ferre (2012b), Field validation of cosmic-ray soil moisture sensor using a distributed sensor network, *Vadose Zone J.*, *11*(4), doi:10.2136/vzj2012.0046.

Franz, T. E., M. Zreda, R. Rosolem, and P. A. Ferre (2013), A universal calibration function for determination of soil moisture with cosmic-ray neutrons, *Hydrol. Earth Syst. Sci.*, *17*, 453–460, doi:10.5194/hess-17-453-2013.

Hornbuckle, B., S. Irvin, T. E. Franz, R. Rosolem, and C. Zweck (2012), The potential of the COSMOS network to be a source of new soil moisture information for SMOS and SMAP, *2012 IEEE International Geoscience and Remote Sensing Symposium (IGARSS)*, 1243–1246, doi:10.1109/IGARSS.2012.6351317.

Ivanov, V. Y., S. Fatichi, G. D. Jenerette, J. F. Espeleta, P. A. Troch, and T. E. Huxman (2010), Hysteresis of soil moisture spatial heterogeneity and the 1homogenizing1 effect of vegetation, *Water Resour. Res.*, *46*, W09521, doi:10.1029/2009WR008611.

Knoll, G. F. (2000), *Radiation Detection and Measurement*, John Wiley, Hoboken, N. J.

Pelowitz, D. B. (Ed.) (2005), MCNPX user's manual, version 5, *Rep. LA-CP-05–0369*, Los Alamos Natl. Lab., Los Alamos, N. M.

Rosolem, R., W. J. Shuttleworth, M. Zreda, T. E. Franz, X. Zeng, and S. A. Kurc (2013), The effect of atmospheric water vapor on the cosmic-ray soil moisture signal, *J. Hydrometeorol.* doi:10.1175/JHM-D-12-0120.1, in press.

Scott, R. L., W. L. Cable, and K. R. Hultine (2008), The ecohydrologic significance of hydraulic redistribution in a semiarid savanna, *Water Resour. Res.*, *44*, W02440, doi:10.1029/2007WR006149.

Vereecken, H., T. Kamai, T. Harter, R. Kasteel, J. Hopmans, and J. Vanderborght (2007), Explaining soil moisture variability as a function of mean soil moisture: A stochastic unsaturated flow perspective, *Geophys. Res. Lett.*, *34*, L22402, doi:10.1029/2007GL031813.

Wood, E. F., et al. (2011), Hyperresolution global land surface modeling: Meeting a grand challenge for monitoring Earth's terrestrial water, *Water Resour. Res.*, *47*, W05301, doi:10.1029/2010WR010090.

Zreda, M., D. Desilets, T. P. A. Ferre, and R. L. Scott (2008), Measuring soil moisture content non-invasively at intermediate spatial scale using cosmic-ray neutrons, *Geophys. Res. Lett.*, *35*, L21402, doi:10.1029/2008GL035655.

Zreda, M., W. J. Shuttleworth, X. Xeng, C. Zweck, D. Desilets, T. E. Franz, and R. Rosolem (2012), COSMOS: The COsmic-ray Soil Moisture Observing System, *Hydrol. Earth Syst. Sci.*, *16*, 4079–4099, doi:10.5194/hess-16-1-2012.